Functional network reconfiguration supporting memory-guided attention

Kylie Isenburg [1,2], Thomas M. Morin [1,2], Maya L. Rosen[3], David C. Somers[1,2,4], Chantal E. Stern[1,2,4,*]

[1]Graduate Program for Neuroscience, Boston University, 677 Beacon Street, Boston MA 02215, USA,
[2]Cognitive Neuroimaging Center, Boston University, 610 Commonwealth Avenue, Boston MA 02215, USA,
[3]Program in Neuroscience, Smith College, 100 Green Street, Northampton MA 01063, USA,
[4]Department of Psychological and Brain Sciences, Boston University, 64 Cummington Mall, Boston MA 02215, USA

*Corresponding author: Department of Psychological and Brain Sciences, Boston University, Boston, Massachusetts, 02215, USA. Email: chantal@bu.edu

Studies have identified several brain regions whose activations facilitate attentional deployment via long-term memories. We analyzed task-based functional connectivity at the network and node-specific level to characterize large-scale communication between brain regions underlying long-term memory guided attention. We predicted default mode, cognitive control, and dorsal attention subnetworks would contribute differentially to long-term memory guided attention, such that network-level connectivity would shift based on attentional demands, requiring contribution of memory-specific nodes within default mode and cognitive control subnetworks. We expected that these nodes would increase connectivity with one another and with dorsal attention subnetworks during long-term memory guided attention. Additionally, we hypothesized connectivity between cognitive control and dorsal attention subnetworks facilitating external attentional demands. Our results identified both network-based and node-specific interactions that facilitate different components of LTM-guided attention, suggesting a crucial role across the posterior precuneus and restrosplenial cortex, acting independently from the divisions of default mode and cognitive control subnetworks. We found a gradient of precuneus connectivity, with dorsal precuneus connecting to cognitive control and dorsal attention regions, and ventral precuneus connecting across all subnetworks. Additionally, retrosplenial cortex showed increased connectivity across subnetworks. We suggest that connectivity from dorsal posterior midline regions is critical for the integration of external information with internal memory that facilitates long-term memory guided attention.

Key words: memory; attention; precuneus; fMRI; connectivity.

Introduction

Our attentional capacities are limited, as a very small number of objects can be attended in a moment (Sears and Pylyshyn, 2000; McMains and Somers, 2004; Cavanaugh and Alvarez, 2006), attention can only be switched a few times per second (Weichselgartner and Sperling 1987; Koch et al. 2011), and unattended objects go largely unprocessed (Simons and Chabris, 1999). How can we reconcile these severe limitations of our attentional system with the high level of real-world performance that humans exhibit in complex, but familiar settings? For instance, how does a native New Yorker function so well in the "blooming, buzzing confusion" of Times Square when there are so many stimuli present? A growing body of literature suggests that context-dependent retrieval of long-term memory (LTM) serves to direct resources of attention to the most relevant stimuli and locations (Chun and Jiang 1998; Summerfield et al. 2011; Rosen et al. 2015; 2016; 2018). The brain networks that support LTM and those that support attention are likely in regular communication; however, standard parcellations largely emphasize a segregation of LTM and attention networks and indicate that these networks are anti-correlated (Yeo et al. 2011; Power et al. 2011; Spreng et al. 2013). Long-term memory-guided attention (LTM-guided attention) has been investigated

in neuroimaging studies, which identify several cortical and subcortical structures, including intraparietal sulcus, posterior precuneus, mediodorsal thalamus, and hippocampus that support these processes (Summerfield et al. 2006; Hutchinson and Turk-Browne 2012; McDermott et al. 2017; Rosen et al. 2015; 2016; 2018; Chen and Hutchinson 2019; Gilmore et al. 2021). These findings have created a foundation for understanding the neural underpinnings of LTM-guided attention, but a greater understanding of network interactions is needed. Here, we extend this foundational work by examining both large-scale, network-level and fine-grained, node-level interactions that support the process of LTM-guided attention.

An early study analyzing blood-oxygen-level-dependent (BOLD) signal via functional magnetic resonance imaging (fMRI) compared LTM-guided attention with stimulus-guided (STIM-guided) attention, a visual attentional mechanism guided by the saliency of the external stimulus (Summerfield et al. 2006). While this study found no cortical differences between these two modes of attention, results showed greater hippocampal activation facilitating LTM-guided attention (Summerfield et al. 2006). A similar study conducted more recently by Goldfarb et al. found comparable results, with hippocampal and striatal activation contributing to LTM-guided versus STIM-guided attention (Goldfarb et al. 2016). Work from our lab compared

LTM-guided attention to STIM-guided attention and to memory retrieval (LTM-retrieval) separately and identified several cortical and subcortical regions—posterior precuneus, posterior callosal sulcus, lateral intraparietal sulcus, caudate head, mediodorsal thalamus, and cerebellar lobule VI/Crus I, which we suggested might constitute a Memory-Attention Network (Rosen et al. 2015; 2016; 2018).

Generally, regions identified in these studies fall largely into three canonical brain networks, the dorsal attention network, the cognitive control network, and the default mode network (Yeo et al. 2011). Within these large-scale networks, finer-grain network parcellations have also been identified, splitting the over-arching networks into subnetworks (Power et al. 2011; Yeo et al. 2011). Dorsal attention subnetwork A consists of superior parietal lobe, parietal occipital lobe, and temporo-occipital lobe, while subnetwork B includes postcentral gyrus and frontal eye fields (Yeo et al. 2011). These regions are implicated in visuo-spatial processing and perception and play a role in goal-directed orientation of attention to incoming sensory information (Corbetta and Shulman 2002). Default mode subnetwork A contains medial temporal lobe, a ventral portion of the posterior precuneus, posterior callosal sulcus, and medial prefrontal cortex. Subnetwork B is left lateralized and is considered the language network, composed of ventral and dorsal prefrontal cortex, while subnetwork C holds a posterior segment of the inferior parietal lobule, retrosplenial cortex, and parahippocampal cortex (Yeo et al. 2011). These sub-networks are highly active at rest and are proposed to facilitate self-referential thought (Raichle et al. 1996), internal processing mechanisms, and memory (Raichle and Snyder 2007). Cognitive control subnetwork A holds the inferior bank of the intraparietal sulcus, the inferior prefrontal sulcus, and anterior midcingulate. Subnetwork B is made up of inferior parietal lobe directly adjacent to default mode C, lateral temporal lobe, and dorsolateral and ventrolateral prefrontal cortex. Subnetwork C consists of the posterior precuneus and posterior cingulate cortex/callosal sulcus (Yeo et al. 2011). These regions have been implicated as key nodes of a Memory Attention Network (Rosen et al. 2015; 2016; 2018) and of a Parietal Memory Network (Gilmore et al. 2015).

The goal of our study was to investigate the node- and network-level interactions that support large-scale communication across brain regions to facilitate LTM-guided attention, a task that requires communication between internal mnemonic processing and externally driven attention. As such, we aimed to characterize functional connectivity between nodes of the dorsal attention, cognitive control, and default mode subnetworks, identifying node- to network-level interactions that facilitate LTM-guided attention, versus STIM-guided attention and LTM-retrieval control conditions. We hypothesized that network connectivity would shift based on attentional demands of the task, with greater reliance on nodes within the default mode subnetworks supporting internal demands of LTM-guided attention via increased connectivity with attention-specific nodes from the dorsal attention and cognitive control subnetworks. Additionally, we hypothesized greater connectivity between dorsal attention and cognitive control subnetworks to support external attentional demands. To investigate our hypothesis, we utilized fMRI data previously collected from our lab (Rosen et al. 2018) and performed task-based connectivity using a generalized Psychophysiological Interaction (gPPI) analysis (McLaren et al. 2012). Utilizing a 400-node parcellation atlas (Schaefer et al. 2018) of the 17 canonical resting-state brain networks (Yeo et al. 2011), we conducted a region of interest (ROI) analysis between 192 nodes of the dorsal attention (subnetworks A and

B), cognitive control (subnetworks A, B, and C), and default mode (subnetworks A, B, and C) networks during LTM-guided attention, STIM-guided attention, and LTM-retrieval. We characterized task-based connectivity differences between LTM-guided attention compared to STIM-guided attention to isolate memory recall and attentional deployment demands of the task. Additionally, we contrasted LTM-guided attention > LTM-retrieval to isolate the process of guiding one's attention based on memory, controlling for memory recall itself. Our results explicate network- and node-level characteristics that contribute to attentional mechanisms enhanced by long-term memory.

Methods
Participants
We re-analyzed a previously collected dataset of 25 right-handed, healthy fMRI participants (13 male, ages 22–34) with normal or corrected-to-normal vision (Rosen et al. 2018). The study was approved by the Institutional Review Board of Boston University and participants were recruited and enrolled from Boston University and the greater Boston area. Participants gave written informed consent prior to study participation and completed the study at two separate sessions (training and test). Due to fatigue in the scanner, 1 participant was excluded from all analyses, resulting in 24 participants in the final analysis.

Visual stimuli and experimental paradigm
Experimental sessions were conducted across two consecutive days, beginning with a training session on Day 1 and an fMRI scanning session on Day 2. The main experimental condition was LTM-guided attention, contrasted with two controls: STIM-guided attention and LTM-retrieval. STIM-guided attention was created to match the attentional demands of the LTM-guided condition without components of memory retrieval. LTM-retrieval was designed to match the mnemonic demands of LTM-guided attention while controlling for covert visuospatial attention. Additionally, a baseline condition for visual-motor control was included in the paradigm.

Stimuli consisted of 48 object image categories, each with four exemplar images (192 total images) divided in half into lists A and B (see Rosen et al. 2018 for category examples). Half of the participants (Group A) were presented with List A as target objects for the experimental conditions, while List B was used for distractor and visual-motor control images. The other half of the participants (Group B) were given List B for targets and List A for distractors/control. For both groups, the target list was further divided into three lists of eight object categories to be used in the three experimental conditions (counterbalanced across subjects within each group).

Day 1 (training): participants completed three separate training paradigms for stimuli used in the three different experimental conditions. Training was conducted separately for each condition with order counterbalanced across participants. Exposure to each stimulus was matched across conditions to account for familiarity of stimuli. Training ensured that participants encoded all word-object (LTM-retrieval) and word-location pairings (LTM-guided attention) for accurate performance during the scan. Full details regarding training can be found in greater detail in Rosen et al. 2018.

Day 2 (testing/scanning): the trained tasks were presented during fMRI scanning in a block design (Fig. 1). At the start of each block, a cue indicated the upcoming condition (LTM-guided attention, LTM-retrieval, STIM-guided attention, or visual-motor
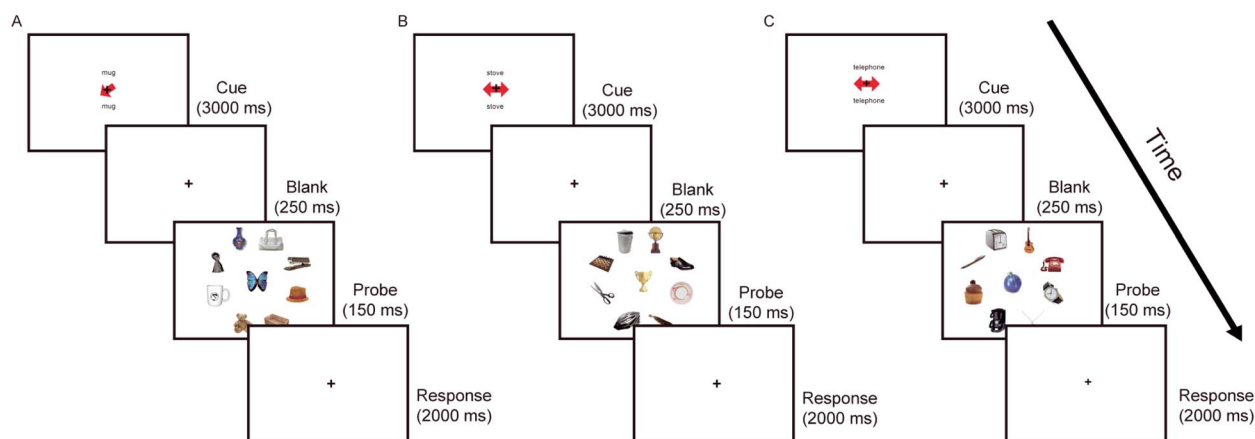
Fig. 1. Participants were trained and later scanned with three separate conditions: A) during STIM-guided attention, a red arrow prompted the participants to direct their attention and indicate whether the object in the location was a match to the named category, B) in the LTM-retrieval condition, the double-sided red arrows were uninformative, and participants had to indicate whether the central object was a paired-associate of the category word by memory, C) for LTM-guided attention, the double-sided arrows were again uninformative, however here participant were instructed to direct their attention to the paired location of the category word, and indicate whether the paired object was in the correct location. Original figure from Rosen et al. 2018, Cerebral Cortex.

control). Each scan consisted of eight blocks, containing eight trials per condition.

Stimulus-guided attention

During the STIM-guided attention task (Fig. 1A), a category word that had not been previously studied was presented on the screen (1.85 s) above and below a fixation cross along with an arrow pointing to one of eight peripheral locations, followed by a blank screen for 1 s. Participants were instructed to maintain fixation while covertly guiding their attention to the cued location. Nine objects (1 at the fixation point and 8 in the periphery locations) appeared for 150 ms, followed by a 2-s window where participants were instructed to respond if the object appearing at the cued location was a match (50% of trials) or non-match to the previously presented category word.

LTM-retrieval condition

For the LTM-retrieval condition (Fig. 1B), a cue word was presented on the screen (1.85 s) above and below a fixation cross alongside an uninformative double-headed arrow, presented to match visual drive across conditions. The presented cue word was studied with an associated object during training. Participants were instructed to retrieve the object associated with the word from memory during a 1-s blank screen, after which an array of nine objects appeared for 150 ms. Following this, during a 2-s response window, participants were instructed to indicate whether the center-screen object was a match (50% of trials) or non-match.

LTM-guided attention

During the LTM-guided attention condition (Fig. 1C), a cue word was presented on the screen for 1.85 s above and below a fixation cross alongside an uninformative double-headed arrow. The cue word had been associated with a paired location on the screen during training. The participants were instructed to retrieve the paired location and direct their attention to that location during a 1-s delay period, after which an array of nine objects appeared on the screen for 150 ms. Following this, during a 2-s response window, participants were instructed to respond as to whether the object that appeared in the location was a match (50% of trials) or

non-match. On non-match trials, the target appeared at one of the alternative seven locations to ensure that participants were not attending to their entire periphery.

Visual-motor control

During the visual-motor control baseline condition, participants saw the word "passive" above and below a fixation cross. After a blank screen, nine objects appeared, and the participants were instructed to randomly press a button. The same nine objects appeared in different configurations in every control trial.

MR data acquisition

MRI data were collected on a 3 Tesla Siemens TIM Trio MR scanner located at the Center for Brain Science at Harvard University in Cambridge, MA. Data were acquired using a 32-channel head coil. Functional data were collected using a T2*-weighted echo planar imaging (EPI) sequence with simultaneous multi-slice (SMS) acquisition using the blipped-CAIPI technique (Setsompop et al. 2012) (TR/TE = 2 s/30 ms, flip angle = 80°, bandwidth = 1,596 Hz/px, number of slices = 65, acceleration factor = 3, voxel size = 2 mm isotropic). Each participant completed between 9 and 12 functional scan runs (191 volumes, 6 min 22 s) during one scan session, with each run containing eight task blocks, two of each condition. Structural MRI were collected using high-resolution T1-weighted multi-planar rapidly acquired gradient echo (MPRAGE) images (TR/TE = 2.2 s/1.54 ms, flip angle = 7°, resolution = 1.0 × 1.0 × 1.3 mm). Seventeen of the participants completed structural scans at the same facility as their functional scans, while seven were acquired on an identical scanner and coil at the Martinos Center for Biomedical Imaging, Massachusetts General Hospital, Charlestown MA.

MR data preprocessing

MR data were organized using the Brain Imaging Data Structure (Gorgolewski et al. 2016) and preprocessed using the standard pipeline available in fMRIPrep v1.4.1, a Nipype v1.2.0-based tool (Esteban et al. 2019). Preprocessing included skull stripping, brain surface segmentation and reconstruction, slice timing correction, motion correction, spatial registration of the functional data to each subject's structural T1w scan, and spatial normalization
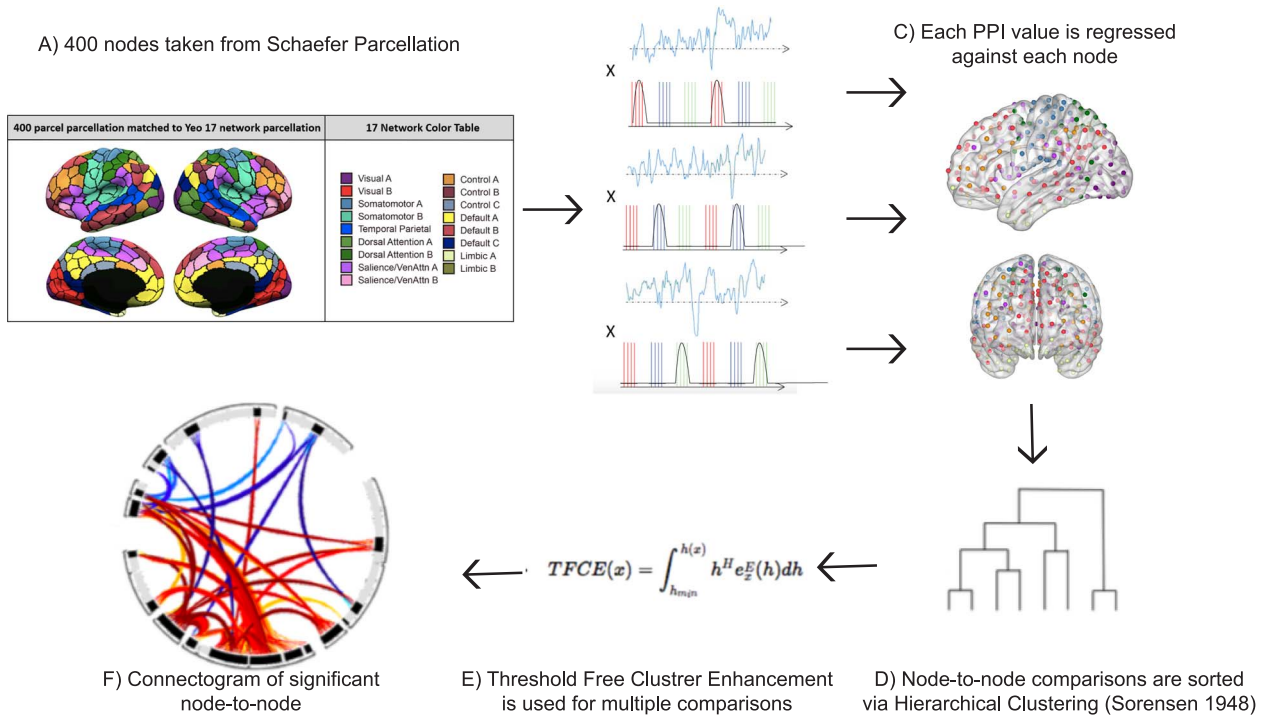
Fig. 2. Step by step method of gPPI analysis implemented in Conn toolbox. A) an inflated image of the 400 cortical nodes matched to the Yeo 17-network atlas (adapted with permission from https://github.com/ThomasYeoLab/CBIG/tree/master/stable_projects/brain_parcellation/Schaefer2018_LocalGlobal). B) A representation of the psychophysiological index regressors utilized in the gPPI analysis. For each of the three conditions, LTM-guided attention, STIM-guided attention, and LTM-retrieval, the block design was multiplied by the time-series of each of the 400 nodes separately to create individual PPI regressors. C) each PPI regressor is used to compute beta values for all possible pairwise comparisons amongst the 400 nodes. D) Beta values were extracted and sorted using hierarchical clustering available in Conn toolbox. This clustering method groups nodes together based on functional similarity and anatomical proximity. E) Threshold free cluster enhancement (TFCE) with $P < 0.01$ is run to correct each node-to-node connectivity pair for multiple comparisons. F) a node-to-node connectogram is constructed within Conn toolbox that displays clusters of connections between ROIs that pass TFCE correction.

of the structural and functional data to the MNI template (MNI152Lin2009cAsym). Several confounding time-series were calculated based on the framewise displacement (FD), DVARS, and two region-wise global signals extracted within the cerebrospinal fluid and white matter. Scans with >3-mm rotation, translation, or FD were excluded from analyses, resulting in the removal of one run. More details on fmriprep steps and the packages used for each are listed in the Supplementary Materials Section 1.

MR data analysis

To compute condition-dependent functional connectivity between canonical brain networks, we used a general Psychophysiological Interaction (gPPI) model (McLaren et al. 2012) implemented in CONN Toolbox (www.nitrc.org/projects/conn; Whitfield-Gabrieli and Nieto-Castanon 2012; Nieto-Castanon 2020). As a first step, spatial smoothing (5-mm spherical kernel) was performed before the denoising process. Outputs from fMRIPrep confounds were selected as first-level covariates, including six motion parameters and their first-order derivatives, outlier volumes, CSF, and WM. Data denoising included these five confounds, the effects of each condition (LTM-guided attention, memory retrieval, stimulus-guided attention, fixation period, block cue, and visual-motor control), linear detrending. Band pass filtering (0.008–0.09 Hz) was performed after nuisance regression.

The gPPI model consisted of a design matrix with the following regressors: (i) the condition regressors formed by convolving the boxcar function of the condition block with the hemodynamic response function (HRF), (ii) a BOLD time series regressor

extracted from each node, and (iii) the main regressor of interest, a PPI value for each condition and node, created via point-by-point multiplication of the first two regressors (A × B) (Fig. 2A). We defined nodes using the Schaefer 400 parcellation brain atlas of the Yeo 17 networks (Schaefer et al. 2018) and employed a node-to-node connectivity analysis on all 24 subjects using a bivariate regression with the aforementioned regressors (Fig. 2B). Pairwise beta values were computed for every possible combination of node pairings, based on regressing each PPI value against each node's time course for each condition. This was followed by group-level averaging across conditions (STIM-guided attention, LTM-retrieval, and LTM-guided attention). Beta values represent changes in functional connectivity between two nodes modulated by the experimental condition over and above connectivity solely related to task-activations alone.

Two contrasts were generated (LTM-guided attention > STIM-guided attention and LTM-guided attention > LTM-retrieval) and connectivity between nodes of the default mode, cognitive control, and dorsal attention subnetworks were compared using connectograms generated with CONN Toolbox. Significant clusters of node-to-node connections were sorted using a fast optimal leaf ordering technique, which uses hierarchical clustering to sort each connection into a cluster based on functional similarity (Bar-Joseph et al. 2001). Clusters were then corrected for multiple comparisons via Threshold Free Cluster Enhancement (TFCE; Smith and Nichols 2009) after 1,000 permutations of the data to compute for each cluster of connections a peak-level family wise error (FWE)-corrected P-value ($P < 0.01$).
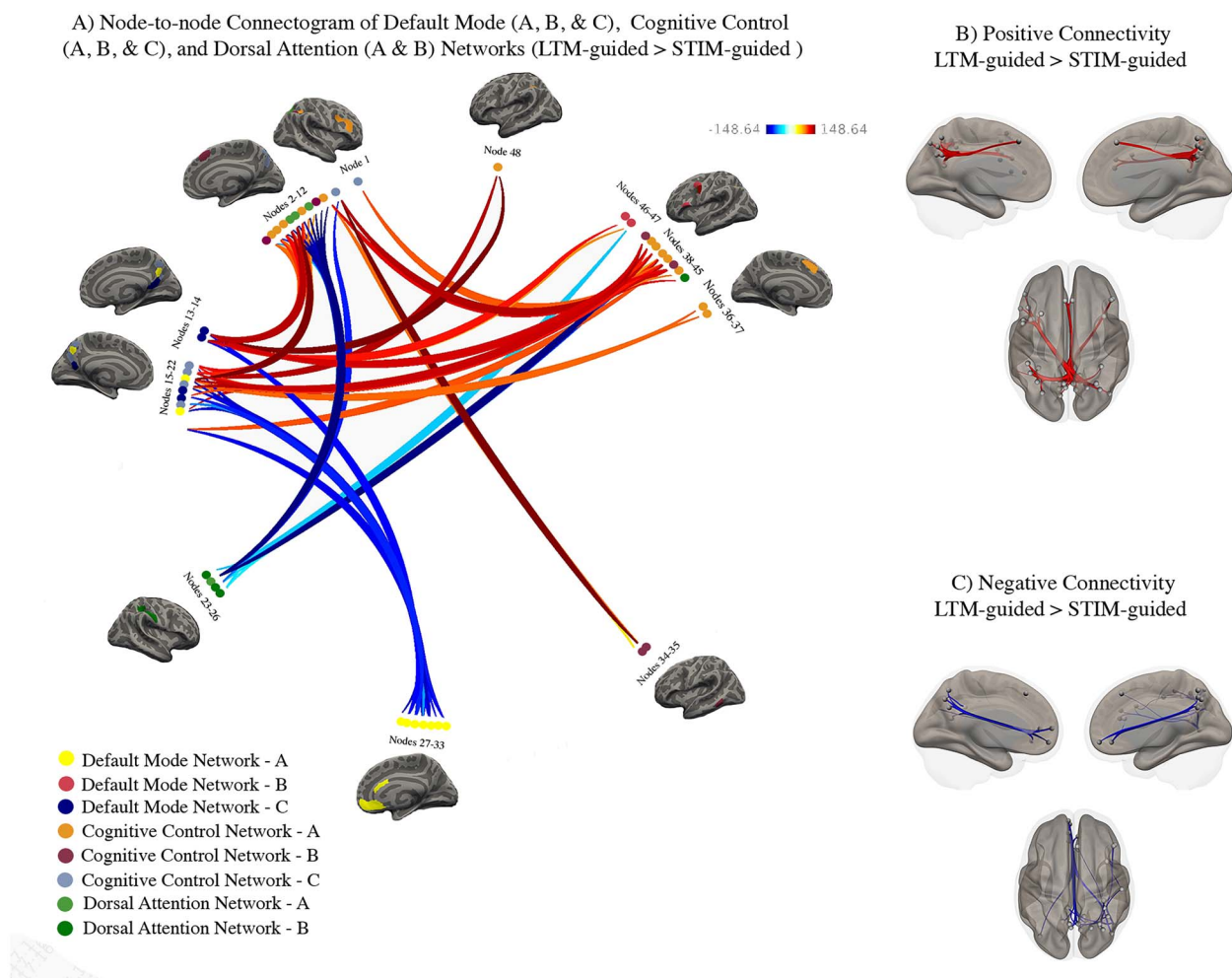
Fig. 3. Condition-modulated connectivity between default mode, cognitive control, and dorsal attention network nodes (LTM-guided attention > STIM-guided attention). A) Significant increases in node-to-node connectivity are shown in red/orange while significant decreases are shown in blue. Darker colors signify stronger task-modulated connectivity between nodes. Inflated brains beside clusters of nodes offer visualization of the nodes and the Yeo 17-network that they belong to. B) Visualization of node-specific locations and the significant positive connections from all clusters. C) Visualization of node location and the significant negative connections from all clusters.

Results

Long-term memory-guided attention versus stimulus-guided attention

We compared task-based functional connectivity during LTM-guided attention contrasted with STIM-guided attention to elucidate mechanisms supporting memory-assisted attentional deployment. Task-based connectivity was computed between 192 nodes from the Schaefer 400 parcellation atlas comprising 8 subnetworks of the default mode, cognitive control, and dorsal attention networks. We identified 48 nodes, (default mode A–9, B–2, C–4; cognitive control A–13, B–6, C–6; dorsal attention A–4, B–4) that displayed significant changes in connectivity with one another for these contrasts. These nodes and their connections are displayed as a connectogram in Fig. 3A. Nodes belonging to each subnetwork are color-coded and numbered along the diameter of the connectogram. For the names of the specific nodes that can be mapped onto the connectogram, see Table 1. From these nodes, we identified 139 significant connections (p-FWE < 0.01) grouped into 12 main clusters that were automatically sorted using Bar-Joseph et al'.s optimal leaf ordering algorithm implemented into CONN toolbox (Bar-Joseph et al. 2001). It is important to note that individual nodes can belong to more than one cluster, and several nodes have multiple connections with varying levels of significance. Clusters of significant increases and decreases in connectivity are summarized in Supplementary Tables 1A and 1B, respectively, and detailed below.

Of seven clusters with increases in connectivity, five showed increased connectivity between posterior default mode subnetwork with various nodes of the cognitive control and dorsal attention subnetworks. Specifically, major default mode contributions stemmed from the posterior precuneus in subnetwork A and the inferior parietal lobe and retrosplenial cortex in subnetwork C. Increased connectivity was noted between default mode A bilateral precuneus and parietal sulcus and prefrontal cortex of cognitive control A (TFCE > 148.64, $P \leq 0.008$). Additionally, the same precuneus nodes exhibit increases in connectivity with the superior parietal lobe of dorsal attention A and the precentral ventral cortex of dorsal attention B (TFCE $\geq$ 146.26, $P \leq 0.000001$). Bilateral retrosplenial nodes from default mode C also increased their connectivity with all subnetworks of the cognitive control network, including lateral prefrontal cortex and inferior parietal sulcus of cognitive control A (TFCE $\geq$ 146.36, $P \leq 0.001$), and inferior parietal lobe of cognitive control B (TFCE $\equiv$ 146.36, $P < 0.000001$).

Table 1. Node labels Fig. 3A.

Default mode (DMN), cognitive control (CCN), dorsal attention (DAN)
left hemisphere (LH), right hemisphere (RH)

1. LH precuneus 2—CCN C	25. RH postcentral gyrus 5—DAN B
2. RH precuneus 5—CCN C	26. RH postcentral gyrus 2—DAN B
3. RH inferior parietal sulcus 1—CCN A	27. RH medial prefrontal 6—DMN A
4. RG inferior parietal lobe 4—CCN B	28. RH medial prefrontal 1—DMN A
5. RH superior parietal lobe 4—DAN A	29. RH medial prefrontal 2—DMN A
6. RH inferior parietal sulcus 4—CCN A	30. RH medial prefrontal 4—DMN A
7. RH superior parietal lobe 5—DAN A	31. LH medial prefrontal 3—DMN A
8. RH superior parietal lobe 2—DAN A	32. LH medial prefrontal 1—DMN A
9. RH lateral prefrontal 5—CCN A	33. LH precuneus 3—DMN A
10. RH lateral prefrontal 3—CCN A	34. LH dorsal prefrontal 1—CCN B
11. RH lateral prefrontal 1—CCN A	35. LH temporal lobe 2—CCN B
12. RH medial prefrontal 1—CCN B	36. LH inferior parietal sulcus 4—CCN A
13. LH retrosplenial 3—DMN C	37. LH lateral prefrontal 1—CCN A
14. RH retrosplenial 2—DMN C	38. LH precentral ventral 1—DAN B
15. RH precuneus 1—CCN C	39. LH ventrolateral prefrontal 1—CCN A
16. LH precuneus 1—CCN C	40. LH medial prefrontal 1—CCN B
17. RH precuneus 2—DMN A	41. LH lateral prefrontal 3—CCN A
18. RH precuneus 2—CCN C	42. LH lateral prefrontal 2—CCN A
19. RH inferior parietal lobe 2—DMN C	43. LH inferior parietal sulcus 1—CCN A
20. RH inferior parietal lobe 1—DMN C	44. LH inferior parietal sulcus 3—CCN A
21. LH precuneus 3—CCN C	45. LH inferior parietal lobe 3—CCN B
22. LH precuneus 6—DMN A	46. LH lateral prefrontal 2—DMN B
23. RH postcentral gyrus 1—DAN B	47. LH ventral prefrontal 3—DMN B
24. RH parieto-occipital 1—DAN A	48. LH inferior parietal sulcus 5—CCN A

We also found nodes stemming from the dorsal precuneus within cognitive control C that exhibited increases in connectivity primarily within-network, and with the dorsal attention subnetworks. Specifically, these nodes showed increased connectivity with the lateral prefrontal cortex of cognitive control A (TFCE ≥ 91.79, $P < 0.008$), dorsal and medial prefrontal cortex of cognitive control B (TFCE ≥ 97.97 m $P < 0.006$), and inferior parietal lobe of cognitive control B (TFCE ≥ 120.45, $P < 0.001$). These nodes also exhibited increased connectivity to the superior parietal lobe of dorsal attention A and the precentral ventral lobe of dorsal attention B (TFCE $= 148.64$, $P < 0.000001$). Apart from these few nodes in the superior parietal lobe of subnetwork A and the precentral ventral cortex of subnetwork B, the dorsal attention network largely showed decreases in connectivity in this contrast.

Nodes shown as having increased connectivity with one another are mapped onto an inflated cortical brain in Fig. 3B. Robust within-network decreases in default mode connectivity were noted between bilateral precuneus and medial prefrontal and inferior parietal nodes (TFCE ≥ 93.78, $P < 0.008$). Notably, these decreases were also apparent within-subnetwork, as medial prefrontal nodes and precuneus nodes both fall within default mode A. Several nodes from the parieto-occipital lobe of dorsal attention A and the postcentral gyrus of dorsal attention B showed decreased connectivity with cognitive control subnetworks. From the parieto-occipital lobe, there was decreased connectivity with lateral/medial prefrontal and inferior parietal sulcus of cognitive control A (TFCE ≥ 92.15, $P < 0.008$), and precuneus nodes of cognitive control C (TFCE $= 145.40$, $P < 0.00001$). Nodes from postcentral gyrus of dorsal attention B decreased connectivity with the inferior parietal sulcus of cognitive control A (TFCE ≥ 92.15, $P < 0.008$) and the precuneus of cognitive control C (TFCE $= 145.40$, $P < 0.00001$). Nodes and connections showing decreased connectivity are mapped onto an inflated cortical brain in Fig. 3C.

A group of nine nodes located along the posterior axis of the precuneus, within default mode A and cognitive control C, exhibited the increased connectivity across cognitive control and dorsal attention subnetworks. These nodes largely span the ventral portion of the posterior precuneus, just superior to the posterior cingulate cortex, spreading into more dorsal regions and crossing the border into the Schaefer division of cognitive control C. Along with retrosplenial cortex, connections including these nodes make up 70% of all significant connectivity results within this contrast, highlighting the importance of default mode subnetworks, and the precuneus in differentiating LTM-guided attention from STIM-guided attention.

Long-term memory-guided attention versus long-term memory retrieval

We compared task-based functional connectivity during LTM-guided attention with LTM-retrieval to control for memory recall and highlight the neural mechanisms facilitating attentional deployment based on memory. This contrast resulted in 96 nodes (default mode A–12, B–10, C–6; cognitive control A–19, B–13, C–8; dorsal attention A–17, B–11) exhibiting significant changes in connectivity with one another. These nodes and their connections are displayed as a connectogram in Fig. 4A. Nodes belonging to each network are color-coded and numbered along the diameter of the connectogram. For the names of the specific nodes that can be mapped onto the connectogram, see Table 2. From these nodes, we identified 399 significant connections, grouped into 38 clusters (p-FWE < 0.01). It is important to note that individual nodes can belong to more than one cluster, as several nodes have multiple connections with varying levels of significance. Clusters of significant increases and decreases in connectivity are summarized in Supplementary Tables 2A and 2B, respectively, respectively, with the most prominent connections detailed below.

Table 2. Node labels Fig. 4A.

Default mode (DMN), cognitive control (CCN), dorsal attention (DAN)
left hemisphere (LH), right hemisphere (RH)

1. RH inferior parietal sulcus 2—CCN A	34. RH frontal eye fields 2—DAN B	65. RH inferior parietal lobe 4—CCN B
2. RH postcentral gyrus 3—DAN B	35. RH frontal eye fields 3—DAN B	66. RH superior parietal lobe 4—DAN A
3. LH inferior parietal sulcus 2—CCN A	36. LH ventrolateral prefrontal—CCN B	67. RH inferior parietal sulcus 1—CCN A
4. LH precuneus 5—DMN A	37. LH inferior parietal lobe 1—CCN B	68. RH superior parietal lobe 2—DAN A
5. LH precuneus 4—DMN A	38. LH inferior parietal lobe 2—CCN B	69. RH superior parietal lobe 5—DAN A
6. RH medial prefrontal 3—DMN A	39. LH temporal lobe 2—CCN B	70. RH inferior parietal lobe 4—CCN A
7. RH medial prefrontal 1—DMN A	40. LH inferior parietal lobe 3—CCN B	71. RH dorsolateral prefrontal 3—CCN B
8. LH medial prefrontal 2—DMN A	41. LH ventrolateral prefrontal 1—CCN A	72. RH lateral prefrontal 2—CCN A
9. LH medial prefrontal 4—DMN A	42. LH medial prefrontal 1—CCN B	73. RH lateral prefrontal 5—CCN A
10. LH medial prefrontal 3—DMN A	43. LH lateral prefrontal 2—CCN A	74. RH lateral prefrontal 1—CCN A
11. LH medial prefrontal 1—DMN A	44. LH lateral prefrontal 3—CCN A	75. RH lateral prefrontal 3—CCN A
12. LH precuneus 3—DMN A	45. LH inferior parietal lobe 1—CCN B	76. RH medial prefrontal 1—CCN B
13. RH precuneus 5—DMN A	46. LH inferior parietal lobe 3—CCN B	77. LH precuneus 2—CCN C
14. RH inferior parietal lobe 1—DMN A	47. LH ventral prefrontal 1—DMN B	78. RH precuneus 5—CCN C
15. LH dorsal prefrontal 1—DMN B	48. LH lateral prefrontal 2—DMN B	79. RH precuneus 2—CCN C
16. LH dorsal prefrontal 4—DMN B	49. LH ventral prefrontal 2—DMN B	80. RH occipitotemporal lobe 1—DAN A
17. LH dorsal prefrontal 2—DMN B	50. LH ventral prefrontal 4—DMN B	81. LH occipitotemporal lobe 2—DAN A
18. RH precuneus 2—DMN A	51. LH dorsal prefrontal 6—DMN B	82. LH parieto-occipital lobe 2—DAN A
19. LH precuneus 3—CCN C	52. LH ventral prefrontal 3—DMN B	83. LH superior parietal lobe 1—DAN A
20. RH precuneus 3—CCN C	53. LH ventral prefrontal 1—DMN B	84. LH superior parietal lobe 3—DAN A
21. RH precuneus 1—CCN C	54. LH temporal lobe 1—CCN A	85. LH superior parietal lobe 6—DAN A
22. LH precuneus 1—CCN C	55. LH inferior parietal sulcus 4—CCN A	86. LH superior parietal lobe 7—DAN A
23. LH retrosplenial 2—DMN C	56. LH inferior parietal sulcus 5–CCN A	87. LH superior parietal lobe 5—DAN A
24. LH retrosplenial 3—DMN C	57. LH occipitotemporal lobe 3—DAN A	88. LH superior parietal lobe 4—DAN A
25. RH retrosplenial 2—DMN C	53. LH postcentral gyrus 2—DAN B	89. LH occipitotemporal lobe 4—DAN A
26. LH inferior parietal lobe 1—DMN C	54. LH postcentral gyrus 3—DAN B	90. LH frontal eye fields 1—DAN B
27. LH dorsal prefrontal 1—CCN B	58. LH lateral prefrontal 1—CCN A	91. LH frontal eye fields 3—DAN B
28. LH postcentral gyrus 7—DAN B	59. LH ventral prefrontal 2—CCN A	92. RH frontal eye fields 1—DAN B
29. RH inferior parietal lobe 2—DMN C	60. LH frontal eye fields 2—DAN B	93. RH superior parietal lobe 6—DAN A
30. RH inferior parietal lobe 1—DMN C	61. RH dorsolateral prefrontal 4—CCN B	94. RH superior parietal lobe 7—DAN A
31. RH precuneus 4—CCN C	62. RH dorsal prefrontal 1—CCN A	95. RH parieto-occipital lobe 3—DAN A
32. RH postcentral gyrus 6—DAN B	63. RH dorsolateral prefrontal 1—CCN B	96. RH superior parietal lobe 1—DAN A
33. RH superior parietal lobe 8—DAN A	64. RH dorsolateral prefrontal 2—CCN B	

For a full list of node-to-node connections falling under each cluster, see Supplementary Table 2.

Widespread, cross-subnetwork increases in connectivity were noted in this contrast. Specifically, increased dorsal attention connectivity was much more prominent than in LTM-guided > STIM-guided. From dorsal attention A and B, we noted increased connectivity from the superior parietal lobe and postcentral gyrus with the precuneus and inferior parietal lobe stemming from cognitive control C (TFCE $\geq$ 98.04, $P < 0.00008$) and the lateral prefrontal cortex from cognitive control A (TFCE $\geq$ 120.58, $P < 0.001$). Additionally, the superior parietal lobe exhibited increased connectivity with precuneus nodes within default mode A (TFCE $\geq$ 107.50, $P \leq 0.0003$). Nodes from frontal eye fields in dorsal attention B exhibited increased connectivity with lateral prefrontal cortex of cognitive control A (TFCE $= 545.21$, $P < 0.00001$), the precuneus of cognitive control C (TFCE $\geq$ 130.52, $P < 0.00001$), and the inferior parietal lobe along default mode C (TFCE > 125.18, $P < 0.00001$).

From default mode C, retrosplenial cortex exhibited increased connectivity with nodes across the lateral and medial prefrontal cortex in cognitive control A and B (TFCE $\geq$ 184.02, $P < 0.00001$) and nodes from parieto-occipital cortex in dorsal attention A (TFCE $\geq$ 217.17, $P < 0.00001$). Additionally, nodes extending from dorsal-ventral prefrontal cortex from default mode B had a more prominent role in this contrast, increasing connectivity mainly with the precuneus of cognitive control C (TFCE $\geq$ 207.52, $P < 0.00001$).

A set of nodes along the bilateral inferior parietal lobe and sulcus at the border of cognitive control A and C and default mode C accounted for roughly 42% of the connections in this contrast. These nodes showed increased connectivity across all three networks, including within-network increases in connectivity. In addition to the connections discussed above, increased connectivity was noted from these inferior parietal nodes with lateral prefrontal cognitive control A (TFCE $\geq$ 164.15, $P < 0.00001$), and lateral and dorsal prefrontal default mode B (TFCE $\geq$ 416.07, $P < 0.00001$). Additionally, they displayed increased connectivity with retrosplenial cortex of default mode C (TFCE $\geq$ 130.52, $P < 0.00001$) and precuneus of cognitive control C (TFCE $\geq$ 104.68, $P < 0.00005$).

Decreased connectivity was noted mainly between the cognitive control and default mode subnetworks and within-default mode subnetwork. Specifically, adjacent nodes of the precuneus, split between the two networks, showed decreased connectivity with one another (TFCE $\geq$ 144.92, $P \leq 0.00001$). Additionally, nodes of the prefrontal cortex split between default mode B and cognitive control A and B exhibited decreased connectivity as well (TFCE $= 151.25$, $P \leq 0.00001$). Decreased within-default mode connectivity was also seen, primarily between the inferior parietal lobe and retrosplenial cortex of subnetwork C and the medial prefrontal cortex of subnetwork A (TFCE $= 125.95$, $P < 0.00001$). Nodes and connections that showed decreased connectivity are mapped onto an inflated brain in Fig. 4C.
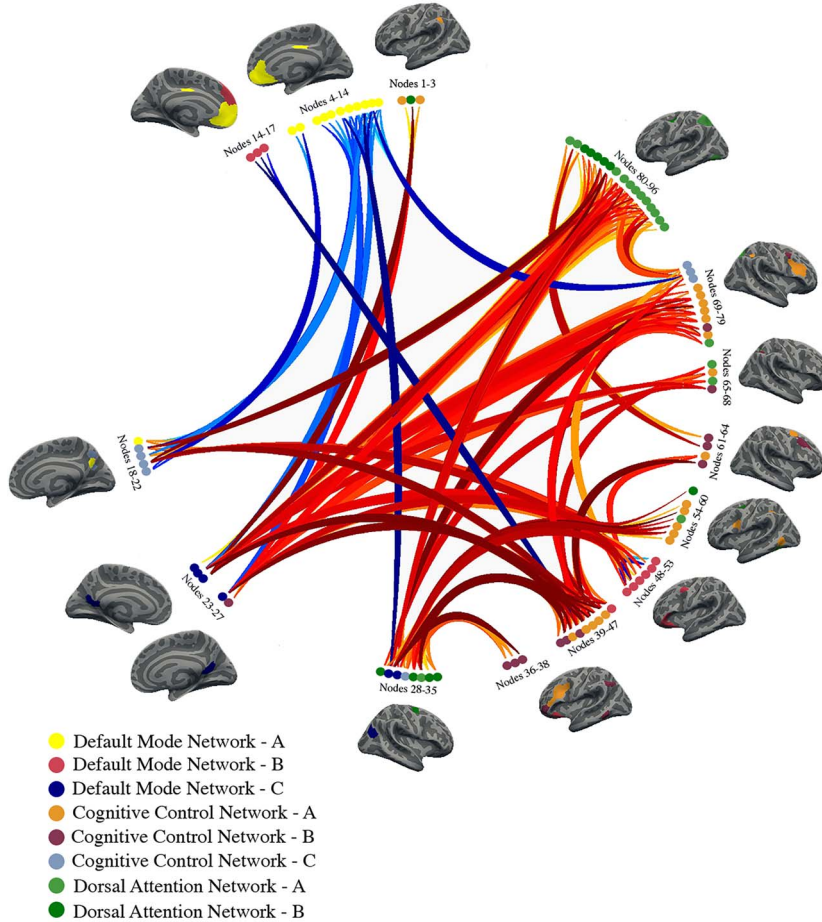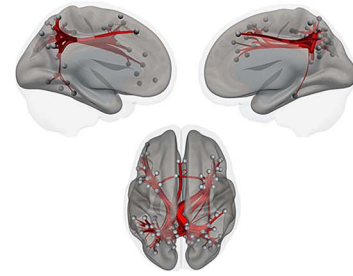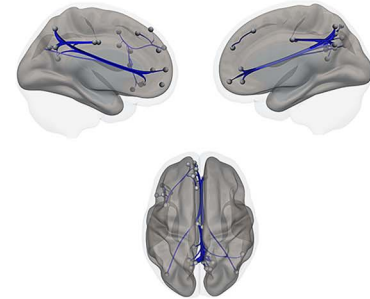
Fig. 4. Condition-modulated connectivity between default mode, cognitive control, and dorsal attention network nodes (LTM-guided attention > LTM-retrieval). A) Significant increases in node-to-node connectivity are shown in red/orange while significant decreases are shown in blue. Darker colors signify stronger task-modulated connectivity between nodes. Inflated brains beside clusters of nodes offer visualization of the nodes and the Yeo 17-network that they belong to. B) Visualization of node-specific locations and the significant positive connections from all clusters. C) Visualization of node location and the significant negative connections from all clusters.

In this contrast, the additional increased connectivity from postcentral gyrus, frontal eye fields, and ventral nodes of the precentral gyrus suggest an increase in dorsal attention network contribution to attentionally demanding components of the task.

Discussion

We investigated how subnetwork- and node-specific functional connectivity facilitates LTM-guided attention in the human brain. Our study identified a specific role for brain regions along the posterior dorsal midline of the brain contributing to LTM-guided attention that persists when controlling for other modes of visually guided attention and memory recall processes. Specifically, we contrasted LTM-guided attention > STIM-guided attention to isolate processes around LTM guided deployment of attention. Here, we noted primary increases in connectivity between posterior regions of cognitive control and default mode subnetworks both within- and across-subnetworks of each overarching network (Fig. 5A), emphasizing the importance for flexible integration between these posterior nodes in facilitating processes specific to the memory demands of the task. We further contrasted LTM-guided attention > LTM-retrieval to isolate attentional demands of the task and saw an increase in integration of

dorsal attention subnetworks with cognitive control subnetworks (Fig. 5B). Therefore, we suggest that across-network communication from dorsal attention regions facilitates the visuo-spatial and attentional demands of the task.

The posterior precuneus and LTM-guided attention

Increased connectivity in both contrasts (LTM-guided attention > STIM-guided attention and LTM-guided attention > LTM-retrieval) was seen along the dorsal-ventral axis of the posterior precuneus spanning into both default mode C and cognitive control C. The strip of the postero-dorsal precuneus identified during LTM-guided > STIM-guided attention is nearly identical to that of the region we found in our previous analysis, identified as part of the cognitive control network (Rosen et al. 2018). Here, we were also able to isolate the portion of the precuneus that falls within the default mode network. This allows for a comprehensive view of activity along the posterior axis of the precuneus that forms a functional gradient beginning above the border of the cognitive control network and traveling ventrally into default mode network. Previous research has found increased functional connectivity between the precuneus and cognitive control brain regions during attentionally demanding tasks (Leech et al. 2012;
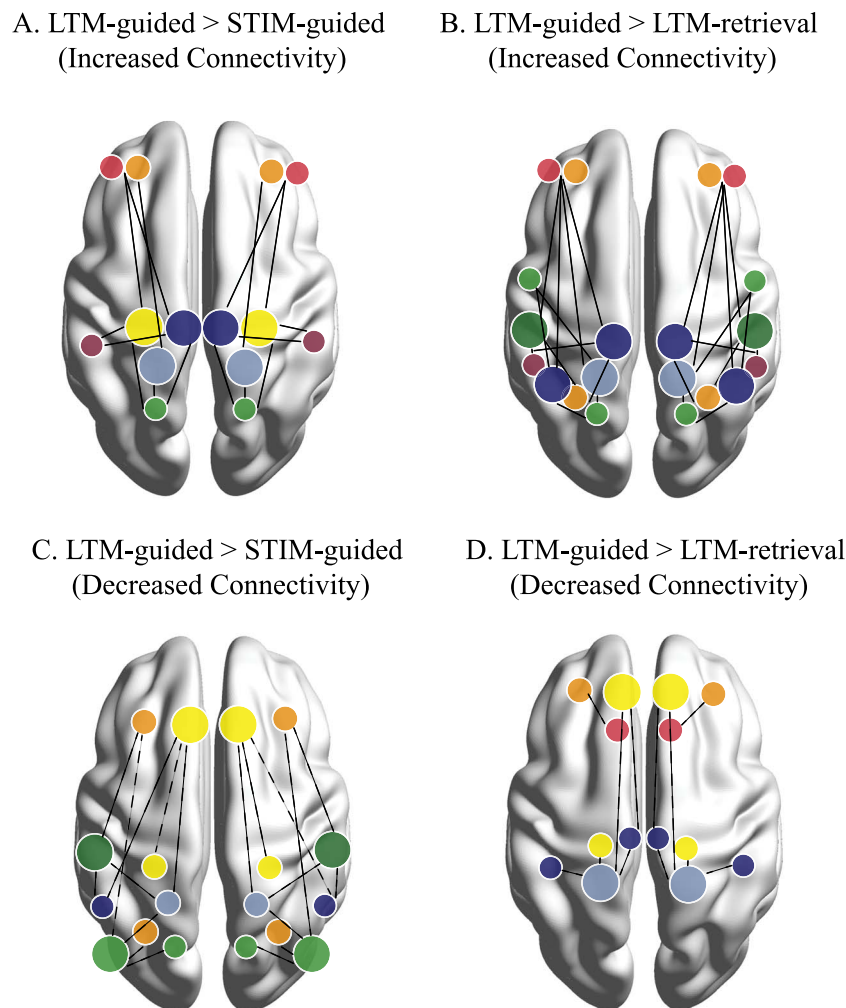
A. LTM-guided > STIM-guided
(Increased Connectivity)

B. LTM-guided > LTM-retrieval
(Increased Connectivity)

C. LTM-guided > STIM-guided
(Decreased Connectivity)

D. LTM-guided > LTM-retrieval
(Decreased Connectivity)

Fig. 5. Conceptual figure illustrating main network interactions resulting from each of the contrasts. Networks are color coded based on the Yeo 17 colors shown in Figs 3 and 4. Prominent nodes of the contrast are denoted by larger dots on the brain. Significant but less recurring nodes are denoted by smaller dots. Solid lines indicate increased connectivity between two nodes for a) LTM-guided > STIM-guided attention, and B) LTM-guided attention > LTM-retrieval. dotted lines indicate decreased connectivity between two nodes for C) LTM-guided > STIM-guided attention, and D) LTM-guided attention > LTM-retrieval. notably, LTM-guided > STIM-guided attention seems to employ connectivity from posterior nodes of the memory-attention network, while LTM-guided attention > LTM-retrieval highlights a role for brain regions involved in visuospatial and external processing.

Utevsky et al. 2014; Li et al. 2019; Lyu et al. 2021). One such study found that reward-based task-performance resulted in increased functional connectivity between the precuneus to left frontal and parietal brain regions within cognitive control network, which decreased during resting-state, as the precuneus integrated back within the default mode network (Utevsky et al. 2014). Our results suggest a similar finding within a distinct sub-region of the precuneus, as the posterior precuneus of default mode C decreases within-network connectivity to medial and lateral prefrontal default mode A and B during the task (Fig. 5C). Additionally, these nodes are less involved in our LTM-guided > LTM-retrieval contrast, and the noted decreased connectivity within-subnetwork no longer persists (Fig. 5D), suggesting that their primary role lies in memory recall. As both contrasts show increased connectivity stemming from the precuneus of cognitive control C, this suggests a critical role of this brain region in long-term memory (LTM-guided > STIM-guided attention), and more specifically in the process of guiding attention based on memory (LTM-guided attention > LTM-retrieval).

The precuneus is a multi-faceted brain region with subdivisions that serve as functionally distinct hubs and is suggested to be a core region of parietal memory networks (Ritchey et al. 2015; Gilmore et al. 2015, 2021; Inhoff and Ranganath 2017;

McDermott et al. 2017; Rosen et al. 2018). In a navigational fMRI study where objects appeared in both consistent and non-consistent locations throughout trajectories, the precuneus was activated
during the consistent object-location condition, supporting object-location memory formation in the parietal cortex (Brodt et al. 2016). Given its implied role in both internally- and externally guided processes, recent work has attempted to functionally subdivide the precuneus. A large-scale analysis of structural, resting-state, and task data found that dorsal and ventral portions of the precuneus operate in causal loops, interpreting external information based on a continuously updated internal model (Lyu et al. 2021). Additionally, they found greater task-based connectivity from the ventral precuneus to brain regions implicated in internal processing (i.e. episodic memory), and greater connectivity from dorsal precuneus to brain regions implicated in cognitive control (Lyu et al. 2021). The precuneus nodes in our results closely align with the divisions identified by Lyu et al., highlighting its role in the internal processing necessary for long-term memory recall.

By combined resting-state functional connectivity analyses from non-human and human primates, Marguilies et al. identified four precuneus subdivisions based on their preferential

connections (Margulies et al. 2009). The precuneus nodes we identify here largely fall into two of the sub-divisions reported by Margulies et al.: the "limbic" and "cognitive" divisions (2009). The Margulies et al. limbic subdivision has connections with brain regions involved in self-referential processing. This subdivision encompasses the most ventral nodes of our precuneus finding, immediately superior to the posterior cingulate, connecting to the lateral prefrontal cortex. The Margulies et al. cognitive subdivision is differentiated based on connections with frontoparietal brain regions implicated in cognitive control and aligns with our postero-dorsal precuneus nodes within cognitive control C. Considering these distinct subdivisions, our results provide further evidence that the posterior precuneus forms a gradient of connectivity from dorsal nodes of the cognitive control network to ventral nodes of the default mode network. We suggest this gradient plays a key role in LTM-guided attention by integrating internal mechanisms of memory with the external processing of incoming visual information necessary for deployment of attention.

Dorsal attention subnetworks facilitate attentional demands

Our previous results identified several brain regions spanning both the cognitive control and the dorsal attention networks facilitating various aspects of LTM- and STIM-guided attention (Rosen et al. 2015; 2016; 2018). In our LTM-guided attention > STIM-guided attention contrast, we note decreased connectivity from postcentral gyrus and superior parietal lobe of the dorsal attention subnetworks A and B with subnetworks across default mode and cognitive control. However, when contrasting LTM-guided attention > LTM-retrieval, we see a prominent role for dorsal attention subnetworks in facilitating attentional demands of the task. The dorsal attention network has been implicated primarily in tasks involving externally directed attention, activating based on goals of the task and the saliency of the stimulus (Corbetta and Shulman 2002). While brain regions from dorsal attention subnetworks play a minimal role in the long-term memory component of LTM-guided attention, isolating the mechanisms whereby attention is deployed results in an increase of dorsal attention node connectivity. Precentral ventral and parieto-occipital nodes from subnetwork A and postcentral gyrus and frontal eye field nodes from subnetwork B showed increased connectivity across subnetworks of the cognitive control network and the default mode network. Our results suggest that contributions from these subnetworks are specifically important for the direction of attention from memory.

Posterior parietal cortex as a relay between internal and external demands

In both contrasts, and most prominently in the LTM-guided > LTM-retrieval contrast, we noted several increases in connectivity from a group of nodes that border the bilateral inferior parietal lobes and sulci along both the cognitive control and default mode networks. Additionally, retrosplenial cortex from default mode C increased connectivity across all canonical brain networks. Combined with our posterior precuneus findings, we suggest a role whereby these posterior midline brain regions facilitate attention towards external spatial locations based on the retrieval of an internal memory representation. This suggestion is in line with anatomical studies of the macaque brain have shown extensive projections between memory-relevant regions of the medial temporal lobes and the posterior parietal cortex, specifically the retrosplenial cortex which is crucial for episodic memory

(Kobayashi and Amaral 2003; 2007), as well as a resting-state connectivity study proposing that the retrosplenial cortex acts as a memory gateway, facilitating communication from the medial temporal lobes to the neocortex, specifically posterior cortical regions of the default mode network (Kobayashi and Amaral 2003; 2007). Additionally, a recent meta-analysis of neuroimaging studies of the retrosplenial cortex identified functional subdivisions whereby anterior regions are associated with episodic memory and posterior regions associated with scene detection and navigational processes (Chrastil et al. 2018). Further, a review of this region (Alexander et al. 2022) aligns well with our suggestion that this and other posterior brain regions (i.e. precuneus) contribute to the balance between external attention and internal memory representation.

Memory-attention network and LTM-guided attention

Our previous research highlighted cognitive control and dorsal attention network contributions to LTM-guided attention. Specifically, activation in posterior precuneus, posterior callosal sulcus, and lateral intraparietal sulcus was found to be stronger during LTM-guided attention than STIM-guided attention (Rosen et al. 2016; 2018). We highlighted these regions in conjunction with a set of bilateral subcortical regions as components of a Memory-Attention Network (Rosen et al. 2018). Our current results emphasize the role of two of these parietal regions, specifically the posterior precuneus of cognitive control C, and lateral intra-parietal area of cognitive control A and C, in increasing cross-network connectivity to facilitate LTM-guided attention. Contrary to our previous findings, in the present analysis we do not find any significant contributions from the posterior callosal sulcus. Previous work from our lab suggests that within the cognitive control network, the posterior callosal sulcus is relatively isolated. Resting-state functional connectivity demonstrated that posterior callosal sulcus is primarily linked to the cognitive control network via connectivity with the lateral parietal sulcus and the posterior precuneus. Results showed very little connectivity with the prefrontal regions of the cognitive control network (Rosen et al. 2016; Supplemental Fig. 2a). In conjunction with the current findings, we suggest that this region might play less of a dominant role, connecting primarily to the to the posterior precuneus, which connects broadly across subnetworks.

Previously, our investigation into default mode-specific regions found no main effects with respect to neural activation during different conditions, with many default mode regions decreasing activation during LTM-guided attention (Rosen et al. 2016). The higher resolution and node-specificity of the current analysis allowed us to examine condition-dependent functional connectivity within subnetworks of the default mode network at a finer scale. Here, we also see a selection of nodes from default mode C more ventrally within the posterior precuneus, extending as far down as retrosplenial cortex, contributing to LTM-guided attention by increasing their connectivity across cognitive control subnetworks in the prefrontal cortex and inferior parietal lobe. Importantly, in our previous results, when contrasting LTM-guided attention > STIM-guided attention, we did observe activation that fills the full boundaries of the posterior precuneus and extends more ventrally into the retrosplenial cortex, aligning with the nodes identified in the present study (Fig. 2A of Rosen et al. 2018).

Additionally, the inferior parietal lobe on the lateral surface holds nodes belonging to default mode C, which are adjacent to nodes of cognitive control B and the inferior parietal sulcus of cognitive control C. These nodes showed widespread changes

in connectivity across subnetworks, primarily in the LTM-guided attention > LTM-retrieval contrast, suggesting that these regions may primarily contribute to the deployment of attention necessary for LTM-guided attention. The fine-grained resolution of the present analysis helps define the roles of neighboring cognitive control and default mode subregions. These findings emphasize a role for our previously proposed Memory-Attention Network (Rosen et al. 2018), which falls within the canonical cognitive control network, and further expands this network to include adjacent nodes from the default network, including the posterior precuneus, lateral inferior parietal lobe, and retrosplenial cortex. These results suggest that nodes from the cognitive control and default mode networks work in concert to support memory- and attention-dynamics relevant for LTM-guided attention and therefore may also contribute to our previously proposed Memory-Attention Network (Rosen et al. 2018).

Conclusions

The present study identifies network-based and node-specific interactions that facilitate different components of LTM-guided attention. We propose that individual nodes of the posterior precuneus facilitate the process of attending to a visual object based on long-term memory. Specifically, task-based connectivity from postero-dorsal and postero-ventral precuneus to nodes within the cognitive control and dorsal attention systems appears to be critical for directing visuo-spatial attention based on memory. We find that the nodes along the ventral region of the precuneus functionally connect to brain regions involved in internal processing, while nodes in the dorsal portion increases functional connectivity to regions involved in cognitive control. Given the decoupling of the posterior precuneus with the rest of the default mode network when controlling for attention and mnemonic demands, respectively, we suggest that this subdivision is important for the integration of external, attentionally driven information with internal, self-referential processes. Additionally, we propose that other posterior parietal brain regions support both internally relevant and externally attentive demands specific for this process. For example, the retrosplenial cortex appears to play a role in memory-relevant processes while the inferior parietal lobes appear to facilitate attentional demands. These findings are in line with literature that supports functionally distinct subnetworks within the canonical resting-state networks that fractionate based on task demands. Additionally, we find evidence that parietal regions of default mode and cognitive control subnetworks work in conjunction to facilitate memory-specific demands. We also found that connectivity between cognitive control and dorsal attention subnetwork underlies the attentional demands required of LTM-guided attention. This study builds off previous work, demonstrating that in addition to differences in functional recruitment, these three networks and their subnetworks exhibit task-related fluctuations in functional connectivity to support LTM-guided attention.

Data availability statement

The data supporting this manuscript will be made available upon reasonable request.

Citation diversity statement

Recent work in several fields of neuroscience has identified a bias in citation practices such that papers from women and other minority scholars are under-cited relative to the number of such papers in the field (Dworkin et al. 2020a; 2020b). Here, we sought to proactively consider choosing references that reflect the diversity of the field in thought, form of contribution, gender, race, ethnicity, and other factors. First, we obtained the predicted gender of the first and last author of each reference by using databases that store the probability of a first name being carried by a woman (Dworkin et al. 2020a). By this measure (and excluding self-citations to the first and last authors of our current paper), our references contain 11.63% woman-woman (first author-last author), 12.51% man-woman, 17.16% woman–man, 58.71% man–man. This method is limited in that (i) names, pronouns, and social media profiles used to construct the database may not, in every case, be indicative of gender identity, and (ii) it cannot account for intersex, non-binary, and transgender people. We look forward to future work that could help us to better understand how to support equitable practices in science.

Author contributions

Kylie Isenburg (Conceptualization, Formal analysis, Writing—original draft, Writing—review & editing), Thomas Morin (Conceptualization, Formal analysis, Writing—original draft, Writing—review & editing), Maya Rosen (Conceptualization, Data curation, Investigation, Writing—original draft, Writing—review & editing), David Somers (Conceptualization, Data curation, Funding acquisition, Investigation, Writing—original draft, Writing—review & editing), and Chantal Stern (Conceptualization, Funding acquisition, Investigation, Writing—original draft, Writing—review & editing).

Supplementary material

Supplementary material is available at *Cerebral Cortex* online.

Funding

Conflict of interest statement: None declared.

References

Alexander AS, Place R, Starrett MJ, Nitz DA, Chrastil ER. Rethinking retrosplenial cortex: perspectives and predictions. *Neuron*. 2022:111:176–189.

Bar-Joseph Z, Gifford DK, Jaakkola TS. Fast optimal leaf ordering for hierarchical clustering. *Bioinformatics*. 2001:17(Suppl 1):S22–S29.

Brodt S, Pöhlchen D, Flanagin VL, Glasauer S, Gais S, Schönauer M. Rapid and independent memory formation in the parietal cortex. *PNAS*. 2016:113(46):13251–13256.

Cavanaugh J, Alvarez BD, Hurtz W. Enhanced performance with brain stimulation:Attentional shift or visual cue. *J Neurosci*. 2006:26(44):11347–11358.

Chen D, Hutchinson JB. What is memory-guided attention? How past experiences shape selective visuospatial attention in the present. *Curr Top Behav Neurosci*. 2019:41:185–212.

Chrastil ER, Tobyne SM, Nauer RK, Chang AE, Stern CE. Converging meta-analytic and connectomic evidence for functional subregions within the human retrosplenial region. *Behavioral Neurosceince*. 2018:132(5):339–355.

Chun MM, Jiang Y. Contextual cueing: implicit learning and memory of visual context guides spatial attention. *Cogn Psychol*. 1998:36(1):28–71.

Corbetta M, Shulman GL. Control of goal-directed and stimulus-driven attention in the brain. *Nat Rev Neurosci*. 2002:3(3):201–215.

Dale AM, Fischl B, Sereno MI. Cortical surface-based analysis: I. *Segmentation and surface reconstruction NeuroImage*. 1999:9(2):179–194.

Dixon ML, de La Vega A, Mills C, Andrews-Hanna J, Spreng RN, Cole MW, Christoff K. Heterogeneity within the frontoparietal control network and its relationship to the default and dorsal attention networks. *Proc Natl Acad Sci*. 2018:115(7):E1598–E1607.

Dworkin JD, Linn KA, Teich EG, Zum P, Shinohara RT, Bassett DS. The extent and drivers of gender imbalance in neuroscience reference lists. *Nat Neurosci*. 2020a:23(8):918–926.

Dworkin JD, Zurn P, Bassett DS. (In)citing action to realize an equitable future. *Neuron*. 2020b:106:890–894.

Esteban O, Markiewicz CJ, Blair RW, Moodie CA, Isik AI, Erramuzpe A, Kent JD, Goncalves M, DuPre E, Snyder M, et al. fMRIPrep: a robust preprocessing pipeline for functional MRI. *Nat Methods*. 2019:16(1):111–116.

Gilmore AW, Nelson SM, McDermott KB. A parietal memory network revealed by multiple MRI methods. *Trends Cogn Sci*. 2015:19(9):534–543.

Gilmore AW, Quach A, Kalinowski SE, González-Araya EI, Gotts SJ, Schacter DL, Martin A. Evidence supporting a time-limited hippocampal role in retrieving autobiographical memories. *PNAS*. 2021:118(12):e2023069118.

Goldfarb EV, Chun MM, Phelps EA. Memory-guided attention: independent contributions of the hippocampus and striatum. *Neuron*. 2016:89(2):317–324.

Gorgolewski KJ, Auer T, Calhoun VD, Craddock RC, Das S, Duff EP, Flandin G, Ghosh SS, Glatard T, Halchenko YO, et al. The brain imaging data structure, a format for organizing and describing outputs of neuroimaging experiments. *Scientific Data*. 2016:3(1):160044.

Hutchinson JB, Turk-Browne NB. Memory-guided attention: control from multiple memory systems. *Trends Cogn Sci*. 2012:16(12):576–579.

Inhoff M, Ranganath C. Dynamic cortico-hippocampal networks underlying memory and cognition: the PMAT framework. *The Hippocampus From Cells To Systems*. 2017:559–589.

Kobayashi Y, Amaral DG. Macaque monkey retrosplenial cortex: II. Cortical afferents. *J Comp Neurol*. 2003:446(1):48–79.

Kobayashi Y, Amaral DG. Macaque monkey retrosplenial cortex: III. Cortical efferents. *J Comp Neurol*. 2007:502(5):810–833.

Koch I, Lawo V, Fels J, Vorländer M. Switching the cocktail party: exploring intentional control of auditory selective attention. *J Exp Psychol Hum Percept Perform*. 2011:37(4):1140–1147.

Leech R, Braga R, Sharp DJ. Echoes of the brain within the posterior cingulate cortex. *J Neurosci*. 2012:32(1):215–222.

Li R, Utevsky AV, Huettel SA, Braams BR, Peters S, Crone EA, van Duijvenvoorde AC. Developmental maturation of the precuneus as a functional core of the default mode network. *J Cogn Neurosci*. 2019:31(10):1506–1519.

Lyu D, Pappas I, Menon DK, Stamatakis EA. A precuneal causal loop mediates external and internal information integration in the human brain. *J Neurosci*. 2021:41(48):9944–9956.

Margulies DS, Vincent JL, Kelly C, Lohmann G, Uddin LQ, Biswal BB, Villringer A, Castellanos FX, Milham MP, Petrides M. Precuneus shares intrinsic functional architecture in humans and monkeys. *Proc Natl Acad Sci*. 2009:106(47):20069–20074.

McDermott KB, Gilmore AW, Nelson SM, Watson JM, Ojemann JG. The parietal memory network activates similarly for true and associative false recognition elicited via the DRM procedure. *Cortex*. 2017:87:96–107.

McLaren DG, Ries ML, Xu G, Johnson SC. A generalized form of context-dependent psychophysiological interactions (gPPI): a comparison to standard approaches. *NeuroImage*. 2012:61(4):1277–1286.

McMains SA, Somers DC. Multiple spotlights of attentional selection in human visual cortex. *Neuron*. 2004:42(4):677–686.

Nieto-Castanon A. *Handbook of fcMRI methods in CONN*. Hilbert Press; 2020.

Power JD, Cohen AL, Nelson SM, Wig GS, Barnes KA, Church JA, Vogel AC, Laumann TO, Miezen FM, Schlaggar BL, et al. Functional network organization of the human brain. *Neuron*. 2011:72(4):665–678.

Raichle ME, Snyder AZ. A default mode of brain function: a brief history of an evolving idea. *NeuroImage*. 2007:37(4):1083–1090.

Raichle ME, Macleod AM, Snyder AZ, Powers WJ, Gusnard DA, Shulman GL. A default mode of brain function. *National Academy of Sciences*. 2001:98(2):676–682.

Ritchey M, Libby LA, Ranganath C. *Cortico-hippocampal systems involved in memory and cognition*; 2015, pp. 45–64.

Rosen ML, Stern CE, Michalka SW, Devaney KJ, Somers DC. Influences of long-term memory-guided attention and stimulus-guided attention on visuospatial representations within human intraparietal sulcus. *J Neurosci*. 2015:35(32):11358–11363.

Rosen ML, Stern CE, Michalka SW, Devaney KJ, Somers DC. Cognitive control network contributions to memory-guided visual attention. *Cereb Cortex*. 2016:26(5):2059–2073.

Rosen ML, Stern CE, Devaney KJ, Somers DC. Cortical and subcortical contributions to long-term memory-guided visuospatial attention. *Cereb Cortex*. 2018:28(8):2935–2947.

Schaefer A, Kong R, Gordon EM, Laumann TO, Zuo X-N, Holmes AJ, Eickhoff SB, Yeo BTT. Local-global parcellation of the human cerebral cortex from intrinsic functional connectivity MRI. *Cereb Cortex*. 2018:28(9):3095–3114.

Sears CR, Pylyshyn ZW. Multiple object tracking and attentional processing. *Can J Exp Psychol*. 2000:54(1):1–14.

Setsompop K, Cohen-Adad J, Gagoski BA, Raij T, Yendiki A, Keil B, Wedeen VJ, Wald LL. Improving diffusion MRI using simultaneous multi-slice echo planar imaging. *NeuroImage*. 2012:63(1):569–580.

Simons DJ, Chabris CF.. Gorillas in our midst:Sustained inattentional blindness for hynamic events. *Perception*. 1999:28(9):1059–1074.

Smith S, Nichols T. Threshold-free cluster enhancement: addressing problems of smoothing, threshold dependence and localisation in cluster inference. *NeuroImage*. 2009:44(1):83–98.

Spreng RN, Sepulcre J, Turner GR, Stevens WD, Schacter DL. Intrinsic architecture underlying the relations among the default, dorsal attention, and frontoparietal control networks of the human brain. *J Cogn Neurosci*. 2013:25(1):74–86.

Summerfield JJ, Lepsien J, Gitelman DR, Mesulam MM, Nobre AC. Orienting attention based on long-term memory experience. *Neuron*. 2006:49(6):905–916.

Summerfield JJ, Rao A, Garside N, Nobre AC. Biasing perception by spatial long-term memory. *J Neurosci*. 2011:31(42):14952–14960.

Utevsky AV, Smith DV, Huettel SA. Precuneus is a functional core of the default-mode network. *J Neurosci*. 2014:34(3):932–940.

Weichselgartner E, Sperling G. Dynamics ofc autonomic and controlled visual attention. *Science*. 1987:238(4828):778–780.

Whitfield-Gabrieli S, Nieto-Castanon A. Conn:a functional connectivity toolbox for correlated and anticorrelated brain networks. *Brain Connectivity*. 2012:2(3):125–141.

Yeo BTT, Krienen FM, Sepulcre J, Sabuncu MR, Lashkari D, Hollinshead M, Roffman JL, Smoller JW, Zöllei L, Polimeni JR, et al. The organization of the human cerebral cortex estimated by intrinsic functional connectivity. *J Neurophysiol*. 2011:106(3):1125–1165.